ACS Macro Letters

pubs.acs.org/macroletters Letter

# All-Polyhydroxyalkanoate Triblock Copolymers via a Stereoselective-Chemocatalytic Route

Andrea H. Westlie, Sarah A. Hesse, Xiaoyan Tang, Ethan C. Quinn, Celine R. Parker, Christopher J. Takacs, Christopher J. Tassone, and Eugene Y.-X. Chen*

Cite This: *ACS Macro Lett.* 2023, 12, 619–625 Read Online

ACCESS | Metrics & More | Article Recommendations | Supporting Information

**ABSTRACT:** Biodegradable polyhydroxyalkanoate (PHA) homopolymers and statistical copolymers are ubiquitous in microbially produced PHAs, but the step-growth polycondensation mechanism the biosynthesis operates on presents a challenge to access well-defined block copolymers (BCPs), especially higher-order tri-BCP PHAs. Here we report a stereoselective-chemocatalytic route to produce discrete hard−soft−hard ABA all-PHA tri-BCPs based on the living chain-growth ring-opening polymerization of racemic (*rac*) 8-membered diolides (*rac*-8DL$^{R}$; R denotes the two substituents on the ring). Depending on the composition of the soft B block, originated from *rac*-8DL$^{R}$ (R = Et, $^{n}$Bu), and its ratio to the semicrystalline, high-melting hard A block, derived from *rac*-8DL$^{Me}$, the resulting all-PHA tri-BCPs with high molar mass ($M_n$ up to 238 kg mol$^{-1}$) and low dispersity ($Đ$ = 1.07) exhibit tunable mechanical properties characteristic of a strong and tough thermoplastic, elastomer, or a semicrystalline thermoplastic elastomer.

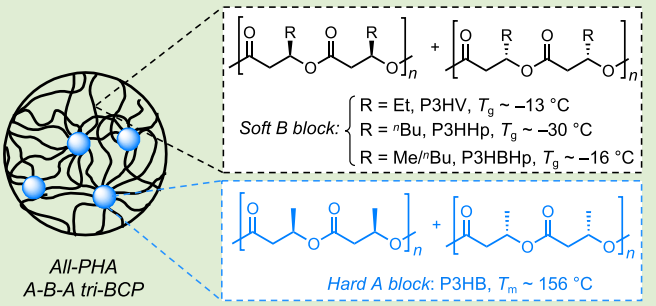


Polyhydroxyalkanoates (PHAs) are natural polyesters that are microbially produced from renewable feedstocks and biodegrade in ambient environments. PHAs offer desired properties as sustainable alternatives to petroleum-based packaging materials.[1−5] However, the biosynthesis of PHAs by microorganisms is limited in several ways: (1) microbes typically produce methyl-substituted PHA (i.e., P3HB) preferentially over PHAs with other pendent substituents; (2) the microbial PHAs are exclusively isotactic (*it*), where all repeat units have an *R* stereoconfiguration; (3) the biosynthesis proceeds via polycondensation of hydroxyacids to produce PHAs in a step-growth mechanism.[6,7] The catalyzed chemical synthesis of PHAs can overcome these limitations and increase the structural diversity of precision PHAs.[8−15] For example, we recently developed a chemocatalytic route based on 8-membered dialkyl diolides, 8DL$^{R}$ [R = Me, Et, $^{n}$Bu, benzyl (Bn)] that addressed these limitations.[16−19] The ring-opening polymerization (ROP) of *rac*-8DL$^{Me}$ results in perfectly *it*-P3HB.[16] Tapered stereoblock copolymers can be produced by the ROP of a diastereomeric mixture of *rac*-8DL$^{Me}$ and *meso*-8DL$^{Me}$.[17] The ROP of a mixture of *rac*-8DL$^{Et}$ and *meso*-8DL$^{Me}$ affords a gradient stereodiblock PHA that exhibits impressive mechanical properties with ultimate tensile strength ($\sigma_b$) = 24.1 ± 1.5 MPa and elongation at break ($\varepsilon_b$) = 564 ± 25%.[17] Polymerization of *meso*-8DL$^{Me}$ with a non-stereoselective catalyst results in syndio-rich PHA, also with impressive mechanical properties.[20] Changing the pendant group to longer alkyl (R = Et, $^{n}$Bu),[18] aromatic (R = Bn),[19] or unsymmetric[21] substituents drastically altered the thermal and mechanical properties of the resulting stereoregular homo- and random PHA copolymers. Another route to toughening PHA copolymers with longer alkyl pendant groups was achieved via carbonylative terpolymerization of a large scope of epoxides and CO using a binary trimetallic Cr$^{III}$ complex/carbonyl cobalt catalyst system.[22,23]

However, more complex polymer architectures, such as triblock copolymers (tri-BCPs), remain largely unexplored for PHAs. Hard−soft−hard ABA tri-BCPs can self-assemble into thermoplastic elastomers (TPEs), an important class of technologically important polymers that combine the elasticity of elastomers and thermal reprocessability of plastics. Tri-BCP-based TPEs typically consist of hard [high glass-transition temperature ($T_g$) and/or high melt-transition temperature ($T_m$)] A blocks and soft (low $T_g$, elastic) B blocks. Aliphatic and degradable polyester-based ABA tri-BCP elastomers with biobased polylactide (PLA) as hard A blocks and various bioderived soft B block polyesters have been reported by Hillmyer et al. and shown to have comparable properties in ultimate tensile stress and elongation at breaks to styrenic BCPs.[24−29] Biosynthetic routes were reported to attain

**Received:** March 17, 2023
**Accepted:** April 19, 2023




https://doi.org/10.1021/acsmacrolett.3c00162
*ACS Macro Lett.* 2023, 12, 619−625

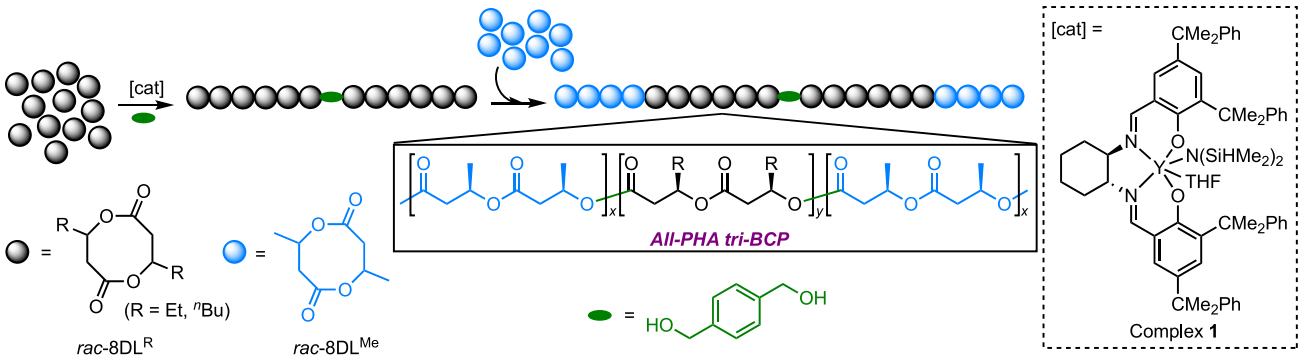


**Figure 1.** Schematic illustration of synthetic pathway to *it*-ABA all-PHA tri-BCPs consisting of the hard *it*-P3HB and soft *it*-P3HHp (or *it*-P3HV and *it*-P3HBHp) blocks.

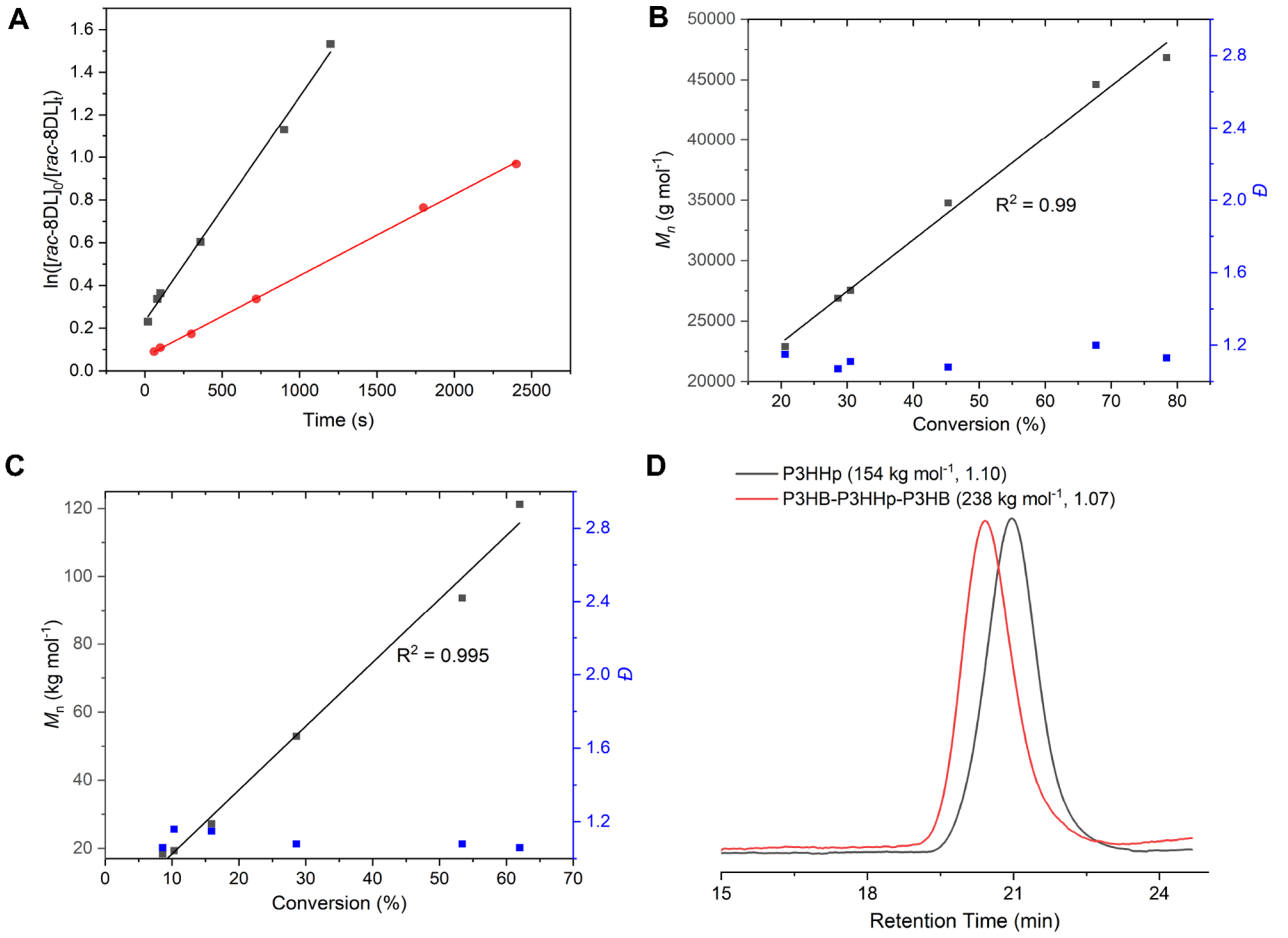


**Figure 2.** Characteristics of the ROP of *rac*-8DL$^{R}$ with complex **1** and BDM. (A) First-order plots of kinetic data up to 40 min; [*rac*-8DL$^{R}$] = 0.5 M. Black line = *rac*-8DL$^{Et}$ and red line = *rac*-8DL$^{Bu}$. (B) Linear relationship between conversion and $M_n$ values for the ROP of *rac*-8DL$^{Et}$; $[BDM]_0$ = 1.22 mM. (C) Linear relationship between conversion and $M_n$ values for the ROP of *rac*-8DL$^{Bu}$; $[BDM]_0$ = 1.22 mM. (D) Representative SEC traces of homopolymer and tri-BCP. Black curve: P3HHp block, $M_n$ = 154 kg mol$^{-1}$, $Đ$ = 1.10; red curve: P3HB-*b*-P3HHp-*b*-P3HB block, $M_n$ = 238 kg mol$^{-1}$, $Đ$ = 1.07.

"blocky" structures consisting of blocks of P3HB and P3HBV [random copolymer of 3-hydroxybutyrate (3HB) and 3-hydroxyvalerate (3HV)] by periodically adding valerate to the bioreactor.[30] However, such blocky P3HB-*b*-P3HBV must be fractionated away from the random copolymer and homopolymer coproducts. The resulting purified biosynthetic BCP displays two $T_m$ values and different tensile profiles compared to the random copolymer.[31] The BCPs containing longer alkyl chains, poly(3-hydroxydodecanoate) (P3HDD) and poly(3-hydroxy-9-decenoate) (P3H9D), were also reported and produced via periodic feeding of an engineered bacterium, although the differential scanning calorimetry (DSC), nuclear magnetic resonance (NMR) evidence, and the total yield of the fractionated BCP remained inconclusive in showing the block regions.[32] Compared to the biosynthetic routes, chemocatalytic routes to PHA BCPs present a vast design space, and some early studies show promising thermomechanical properties of the BCPs. For example,


https://doi.org/10.1021/acsmacrolett.3c00162
ACS Macro Lett. 2023, 12, 619−625

Table 1. Results of Tri-BCPs Synthesized by 1 and BDM in Multi-Gram Scale

| run | midblock | [*rac*-DL$^R$] /[**1**][a] | $M_{n,P3H(V/HHp)}$[b] (kg mol$^{-1}$) | $M_{n,P3HB}$[b] (kg mol$^{-1}$) | $M_{n,total}$[b] (kg mol$^{-1}$) | % midblock[c] | $Đ$[b] ($M_w/M_n$) | $T_m$[d] (°C) | $\Delta H$[d] (J g$^{-1}$) |
|---|---|---|---|---|---|---|---|---|---|
| 1 | P3HV | 600/1 | 84.4 | 59.6 | 144 | 58.6 | 1.14 | 154 | 36.6 |
| 2 | P3HHp | 1800/1 | 154 | 84.0 | 238 | 64.7 | 1.07 | 154 | 42.7 |
| 3 | P3HHp | 700/1 | 172 | 28.0 | 200 | 86.0 | 1.05 | 145 | 8.6 |
| 4 | P3HBHp | 800/1 | 164 | 66.0 | 230 | 71.3 | 1.18 | 156 | 24.3 |

[a]Conditions: carried out at room temperature (RT) in dichloromethane (DCM); precatalyst **1** to BDM initiator ratio fixed at 2:1; see the Supporting Information for detailed conditions for each run. [b]Determined by SEC coupled with an 18-angle light scattering detector at 40 °C in chloroform. [c]% midblock = ($M_{n,P3H(V/HHp)}/M_{n,total}$) × 100. [d]Determined by DSC second heating scan (5 °C/min).

sequential addition or simultaneous polymerization (depending on catalyst) of $\beta$-butyrolactone (BL), which produced the P3HB block, and the benzyl ester functionalized BL, benzyl-$\beta$-malolactone (MLABe), results in a di-BCP that can be postfunctionalized via deprotection of the benzyl ester moiety to produce amphiphilic BCPs.[33] The transamidation reaction of P3HB with polyethylene glycol (PEG) and a primary amine results in di-BCP, P3HB-*b*-PEG.[34] Addition of poly(3-hydroxyoctanoate) (P3HO) to this di-BCP leads to the formation of tri-BCP, P3HB-*b*-PEG-*b*-P3HO, an elastomer that shows promise in biotechnology.[34] ABA tri-BCPs, where the B block is a polycarbonate from cyclopentene oxide (CHO) and $CO_2$ and the A blocks are P3HB from BL, have been synthesized using a one-pot copolymerization of CHO, BL, and $CO_2$ by controlling the $CO_2$ pressure.[35] Di- and tri-BCPs synthesized by sequential addition of (−)-menthide and BL results in microphase separated copolymers and mechanical analysis shows an increase in ductility ($\varepsilon_b$ = 35%) compared to syndiotactic (*st*) P3HB ($\varepsilon_b$ = 18%).[36] A dimethyl substituted benzyl ester PHA copolymer with P3HB has been utilized as the midblock of the tri-BCP with the PLA outer blocks.[37] Recently, we reported the synthesis of an *it*- and *st*-di-BCP, *it*-P3HB-*b*-*st*-P3H4PhB (poly(3-hydroxy-4-phenylbutyrate)), from diastereoselective ROP of *meso*-8DL$^{Bn}$ and *rac*-8DL$^{Me}$.[19] A one-pot synthesis of P3HB-*b*-PCL (polycaprolactone) was similarly achieved, thanks to the catalyst's kinetic preference to polymerize *rac*-8DL$^{Me}$ before $\varepsilon$-caprolactone.[38] Indium-based sequence controlled one-pot copolymerization of BL and $\varepsilon$-decalactone afford di-, tri-, or tetra-BCPs by capitalizing on the monomer relative reactivity ratios.[39]

Here we report the synthesis and characterization of ABA tri-BCP PHAs to access PHA-based TPEs. We reasoned that the highly crystalline, high $T_m$ *it*-P3HB should be a desirable hard A block, and the amorphous, low $T_g$ (−30 °C) butyl-substituted PHA [poly(3-hydroxyheptanoate) (P3HHp)] should be a suitable soft B block, thus furnishing ABA tri-BCP PHA, P3HB-*b*-P3HHp-*b*-P3HB (Figure 1). In addition, the ethyl-substituted PHA [poly(3-hydroxyvalerate) (P3HV)] should also be an appropriate soft B block, as its $T_g$ is about −18 °C,[17] for the construction of another ABA tri-BCP, P3HB-*b*-P3HV-*b*-P3HB. To the best of our knowledge, this structure class is the first example of discrete, *it*-ABA tri-BCPs based completely on 3HBs.

The stereoselective ROP of *rac*-8DL$^R$ is catalyzed by racemic yttrium complexes supported by $C_2$-symmetric *N*,*N*′-bis-(salicylidene)cyclohexanediimine (salcy) ligands.[16−18] To maintain both high catalytic activity and high isoselectivity for the ROP of 8DL$^R$ of contrasting steric bulk, cumyl-substituted Y complex **1** was chosen for the tri-BCP synthesis (Figure 1). This precatalyst, when combined with one equivalent of an alcohol (e.g., benzyl alcohol, BnOH) initiator, undergoes instantaneous alcoholysis to generate the corresponding Y alkoxide catalyst that produces linear homopolymer,[16,18,19] random copolymers,[18,19] or tapered stereodi-BCPs.[17] Since this ROP is a living system, the synthesis of multi-BCPs is then possible through the sequential addition of 8DL$^R$. With a di-initiator such as 1,4-benzenedimethanol (BDM), an ABA tri-BCP is efficiently synthesized via two monomer-addition steps (Figure 1).

In the synthesis, one equivalent of BDM was premixed with two equivalents of precatalyst **1**, and the *in situ* generated active species was added to a B-block monomer. After the ROP of the B-block reached near 100% conversion, the A-block monomer, *rac*-8DL$^{Me}$, was added to furnish a tri-BCP (Figure 1). To demonstrate the livingness, kinetic studies were performed. First, the kinetic plot of each B-block monomer indicates the polymerization is first order in monomer without an induction period (Figure 2A). As expected, the ROP of the sterically more hindered *rac*-8DL$^{Bu}$ is considerably slower than that of *rac*-8DL$^{Et}$. Second, for both B-block monomers, a linear relationship between conversion and molecular weight was observed while dispersity ($Đ$) remains low (between 1.06 and 1.20) throughout the ROP (Figure 2B,C). Third, the size-exclusion chromatography (SEC) trace remained monomodal after polymerization of each block and the observed number-average molar mass ($M_n$) is close to that of the theoretical $M_n$ (Figures 2D and S2−S6). With these lines of evidence showing the living ROP of *rac*-8DL$^{Et}$ and *rac*-8DL$^{Bu}$ using di-initiator BDM, we proceeded with the synthesis of tri-BCPs, P3HB-*b*-P3HV-*b*-P3HB and P3HB-*b*-P3HHp-*b*-P3HB, with P3HV and P3HHp as the soft midblock, respectively. By varying the length of the P3HB hard blocks as well as the length and flexibility of the soft midblock, structure−property relationships for PHA tri-BCPs were unveiled (Table 1).

The well-defined tri-BCP architecture across all formulations was confirmed by three lines of evidence. First, analysis of the resulting tri-BCPs by SEC showed the increased molar mass from the midblock to the tri-BCP as expected while $Đ$ remained monomodal and narrow (Figure 2D and Table 1). For example, the theoretical $M_n$ of the P3HV midblock was 40 kg mol$^{-1}$ (the observed $M_n$ = 60 kg mol$^{-1}$, $Đ$ = 1.07) and the theoretical $M_n$ of resultant tri-BCP was 108 kg mol$^{-1}$ (or 128 kg mol$^{-1}$ based off the observed 60 kg mol$^{-1}$), compared to the observed $M_n$ = 150 kg mol$^{-1}$, $Đ$ = 1.08 (Figure S2). Slightly higher observed molar masses than the calculated ones due to nonquantitative initiator efficiencies is common for this ROP system because of high catalyst sensitivity to adventitious protic impurities brought into the system by the monomer, solvent, and others.[16−19] Second, the carbonyl region of $^{13}C$ NMR spectra showed discrete block formation, without random copolymer formation due to transesterification scrambling of the respective blocks (Figures S7 and S8).


https://doi.org/10.1021/acsmacrolett.3c00162
ACS Macro Lett. 2023, 12, 619−625

Third, diffusion-ordered spectroscopy (DOSY) experiments on a mixture of homopolymers (P3HB and P3HHp) revealed two diffusion coefficients related to each respective polymer (Figure S11), whereas the DOSY experiment on the tri-BCP showed only one diffusion coefficient (Figures S9 and S10), further supporting the formation of the discrete tri-BCP.

The tri-BCP with 58% 3HV incorporation (from *rac*-8DL$^{Et}$) showed two $T_g$ values by DSC: −13 °C for the P3HV block and 5 °C for the P3HB block. The $T_c$ (crystallization temperature) is 58 °C and $T_m$ is 154 °C with an enthalpy of fusion ($\Delta H$) = 36.8 J g$^{-1}$ (Figure 3A). The first heating scan

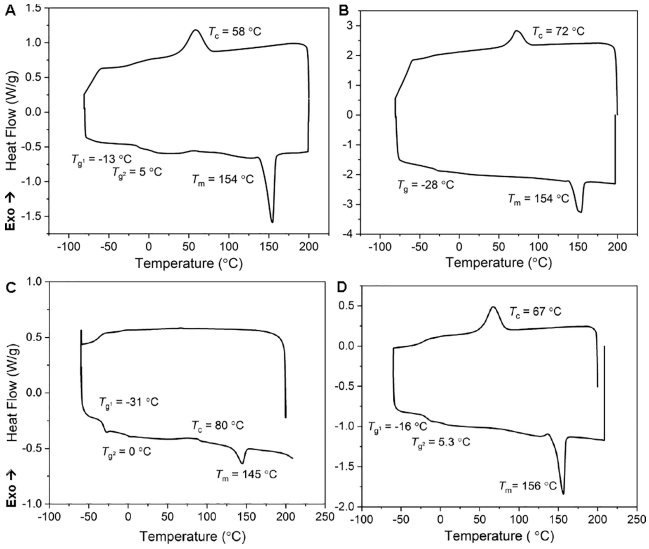


**Figure 3.** Thermal properties of tri-BCPs. DSC curves (first cooling scan from melt and then second heating scan at 5 °C/min) of tri-BCPs produced by **1** (see Table S3 for ROP conditions). (A) P3HB-*b*-P3HV-*b*-P3HB (58% midblock), $\Delta H$ = 36.6 J/g. (B) P3HB-*b*-P3HHp-*b*-P3HB (64% midblock), $\Delta H$ = 42.7 J/g. (C) P3HB-*b*-P3HHp-*b*-P3HB (85% midblock), $\Delta H$ = 8.6 J/g. (D) P3HB-*b*-P3HBHp-*b*-P3HB (66% midblock), $\Delta H$ = 24.3 J/g.

(Figure S1) had two $T_m$ values, 74 °C for P3HV (slow crystallization) and 153 °C for P3HB (fast crystallization), but only the P3HB block $T_m$ peak can be seen on the second heating scan (5 °C/min; Figure 3A). Noteworthy here is that, unlike the random copolymer P3HBV where ∼40% 3HV incorporation resulted in an amorphous material,[18] the tri-BCP with 58% P3HV midblock is still a semicrystalline material with a high $T_m$ of 154 °C.

The tri-BCP with 64% P3HHp midblock (from *rac*-8DL$^{Bu}$) showed one apparent $T_g$ by DSC associated with the P3HHp block, − 28 °C, but a $T_c$ (72 °C) and $T_m$ (154 °C, $\Delta H$ = 42.7 J g$^{-1}$) associated with the P3HB block (Figure 3B). On the other hand, dynamic mechanical analysis (DMA) of this tri-BCP revealed two tan delta peaks at −21.9 and 11.8 °C associated with the P3HHp and P3HB blocks, respectively (Figure S20). In sharp contrast, the random copolymer P3HBHp with ∼60% 3HHp incorporation is an amorphous, viscous liquid that exhibits only a $T_g$ of −30 °C (Figures S12 and S21). Furthermore, increasing the P3HHp midblock to 85% still results in a semicrystalline material with $T_c$ = 80 °C and $T_m$ = 145 °C ($\Delta H$ = 8.6 J/g, Figure 3C). Two $T_g$ values were also observed at −31 °C for the P3HHp block and 0 °C for the P3HB block. To further tune the properties of the final tri-BCP, an amorphous, random copolymer midblock (P3HBHp) was synthesized by statistical copolymerization of *rac*-8DL$^{Me}$ and *rac*-8DL$^{Bu}$ in a 1:1 feed ratio. The resulting tri-BCP P3HB-*b*-P3HBHp-*b*-P3HB (66% midblock) exhibits balanced crystallinity ($T_c$ = 67 °C, $T_m$ = 156 °C with $\Delta H$ = 24.3 J/g) and the expected two $T_g$ values characteristic of the random copolymer (−16 °C) soft block and P3HB hard block (5.3 °C; Figure 3D).

All tri-BCP materials revealed a decomposition temperature at 5% weight loss ($T_d$) between 235−245 °C by thermogravimetric analysis (TGA; Figures S13−S16), typical of PHAs. The melt stability of a representative tri-BCP sample, P3HB-*b*-P3HHp-*b*-P3HB (70% midblock), was investigated first by performing an isothermal hold on TGA at 160 °C under $N_2$ for 45 min to monitor weight loss. Prior to the TGA analysis, all samples were washed by reprecipitation in methanol five times and dried at 50 °C under vacuum for 16 h. During the 45 min isothermal hold, only 1% weight loss was observed (Figure S17). Furthermore, a virgin (nonprocessed) sample was analyzed by DSC via three heating scans. The second heating scan was followed by an isothermal hold for 45 min and then a final cooling and heating scan, which revealed the $T_m$ and $\Delta H$ values remained unchanged (Figure S18). Finally, another virgin sample was subjected to the same TGA isothermal hold as Figure S17, but the $M_n$ and $Đ$ were measured by SEC before and after the isothermal hold. Again, no observed difference in either $M_n$ or $Đ$ was observed (Figure S19). Overall, these controls show polymer degradation is not noticeably observed in the melt under the current conditions. Hence, we proceeded with confidence to examine the mechanical properties of the tri-BCPs by tensile analysis of dog-bone-shaped specimens (ASTM D638 standard, type V).

The tri-BCP with 58% P3HV midblock is a tough thermoplastic with $\sigma_b$ = 26.6 ± 1.4 MPa, elastic modulus ($E$) = 627 ± 63 MPa, and $\varepsilon_b$ = 339 ± 11% (Figure 4A). In contrast, the tri-BCP with 64% P3HHp midblock is an elastomer (no apparent yield point) with $\sigma_b$ = 7 ± 1 MPa, $E$ = 0.45 ± 0.09 MPa, and $\varepsilon_b$ = 290 ± 45% (Figure 4B, red). Increasing the midblock size to 85% resulted in a more elastomeric behavior with $\varepsilon_b$ = 380 ± 67% (Figure 4B, blue). With no observable yield point, this material was subjected to hysteresis (20 cycles, 50% strain), showing elasticity with a 60% elastic recovery (Figure S26). The tri-BCP with the random copolymer P3HBHp midblock is a much stronger thermoplastic, with $\sigma_b$ = 14.7 ± 28 MPa, $E$ = 471 ± 32 MPa, $\varepsilon_b$ = 275 ± 37% (Figure 4B, green). Overall, the effect of the tri-BCP architecture is clearly illustrated by comparing to random copolymer P3HBHp with 40% 3HHp incorporation, which is a much weaker but more flexible ($\varepsilon_b$ ∼ 550%) material (Figure 4B, black), highlighting the importance of architectural control when synthesizing PHAs with desired thermomechanical properties.

Wide-angle X-ray scattering (WAXS) analysis of the tri-BCPs was performed to elucidate the structure−property relationships of these semicrystalline tri-BCP PHAs (Table S9). Figure 5 overlays WAXS profiles of P3HB-*b*-P3HV-*b*-P3HB, 80% P3HV (turquoise), P3HB-*b*-P3HV-*b*-P3HB, 45% P3HV (black), P3HB-*b*-P3HHp-*b*-P3HB, 70% P3HHp (red), and P3HB-*b*-P3HHp-*b*-P3HB, 79% P3HHp (blue). These samples were heated to 160 °C and then allowed to cool to 30 °C. WAXS data shown in Figure 5 were collected from the cooled samples after heat-treatment above the melt (160 °C), as this treatment resembles the specimens on which the mechanical tests were performed. The data taken during heat-


https://doi.org/10.1021/acsmacrolett.3c00162
ACS Macro Lett. 2023, 12, 619−625

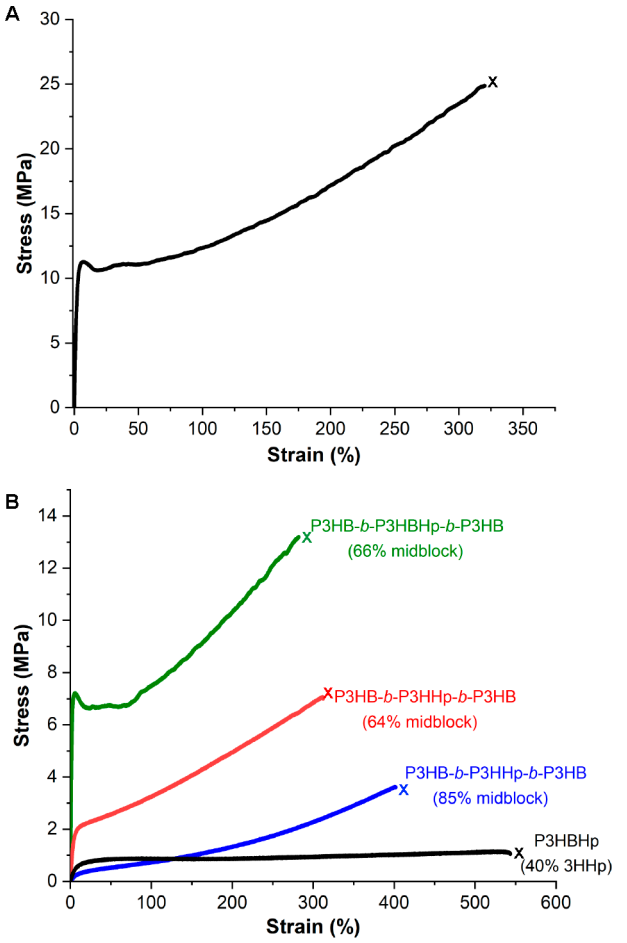


**Figure 4.** Mechanical properties of tri-BCPs. (A) P3HB-*b*-P3HV-*b*-P3HB (58% midblock, $M_n$ = 144 kg mol$^{-1}$). (B) P3HBHp (40% 3HHp units, black ($M_n$ = 144 kg mol$^{-1}$), P3HB-*b*-P3HHp-*b*-P3HB (85% midblock, blue, $M_n$ = 200 kg mol$^{-1}$), P3HB-*b*-P3HHp-*b*-P3HB (64% midblock, red, $M_n$ = 238 kg mol$^{-1}$), P3HB-*b*-P3HBHp-*b*-P3HB (66% midblock, green, $M_n$ = 230 kg mol$^{-1}$).

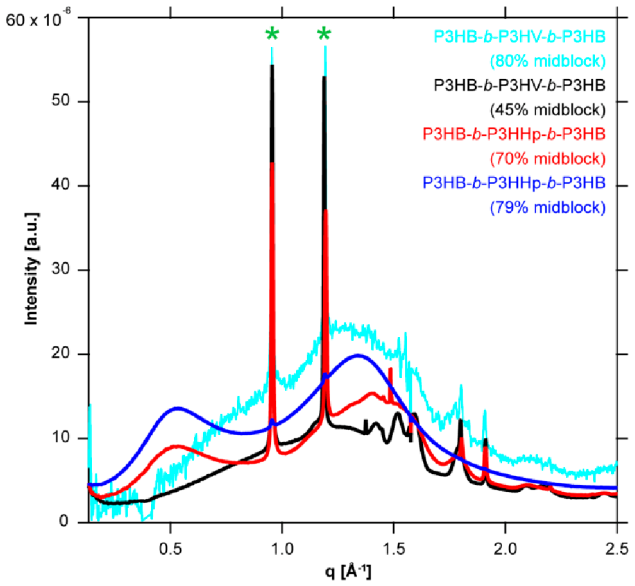


**Figure 5.** WAXS profiles of P3HB-*b*-P3HV-*b*-P3HB, 80% P3HV (turquoise), P3HB-*b*-P3HV-*b*-P3HB, 45% P3HV (black), P3HB-*b*-P3HHp-*b*-P3HB, 70% P3HHp (red), and P3HB-*b*-P3HHp-*b*-P3HB, 79% P3HHp (blue) at 30 °C post-heating to 160 °C. The virgin tri-BCPs were first dissolved in DCM, precipitated into methanol, isolated by filtration, and then dried at 50 °C under vacuum. Intensities between samples are normalized to an intensity at low $q$ in order to visually compare the presence of peaks between samples.

treatment is shown in Figures S22−S25, with corresponding peak fittings summarized in Tables S10−S13.

All samples measured by WAXS show scattering patterns consistent with semicrystalline polymers. To identify which peaks are associated with crystallinity arising from one of the PHA blocks, samples were heated and groupings of peaks that disappeared at specific temperatures were assigned by proximity to the block melting temperature (Figures S22−S25). Since each of the four samples contains a P3HB block and the peaks at $q \sim 0.95$ Å$^{-1}$ (corresponding to a spacing of 6.6 Å) and $q \sim 1.2$ Å$^{-1}$ (corresponding to a spacing of 5.2 Å), marked with a (*) in Figure 5, appeared in all four samples, they were thus assigned to the P3HB block. When looking at the heating data (Figures S22−S25), these peaks either fully disappeared or became weaker as the temperature was increased to 145−160 °C ($T_m$ of P3HB block ∼148 °C). Upon reaching RT post heat-treatment, these peaks reappeared, albeit weaker. A peak around $q \sim 0.91$ Å$^{-1}$ (corresponding to a spacing of 6.9 Å) can be assigned to the P3HV block. This peak disappeared around 100 °C ($T_m$ of P3HV block = 101 °C), and during heating it did not reappear in the cooled sample (due to slow crystallization of P3HV; Figure S22).

Across all samples the degree of crystallinity was reduced following a heat treatment designed to mimic the processing of samples prepared for mechanical testing, as is evident from the loss of a subset of the crystalline peaks and broadening following cooling to RT. The tensile analysis (Figure 4) showed that P3HB-*b*-P3HV-*b*-P3HB is thermoplastic-like, while BCPs with P3HHp midblocks are elastomeric. Additionally, a higher P3HHp content compared to P3HB affords a more elastomeric material. When comparing the mechanical properties to the WAXS data in Figure 5, that is, the post-heating data that is most similar to the compression-molded sample used for tensile testing, it can be hypothesized that the mechanical property differences are a result of the varied degree of crystallinity. From the WAXS data, it is evident that post heating (Figure 5), P3HB-*b*-P3HHp-*b*-P3HB, 79% P3HHp (blue), the BCP with the highest P3HHp content and most similar to the most elastomeric sample (blue trace in Figure 4B), has the weakest crystalline peaks, whereas P3HB-*b*-P3HV-*b*-P3HB, 45% P3HV (black), the sample most similar to the thermoplastic-like sample (Figure 4A), has a more crystalline character. Further studies are underway to understand the correlation between the process history impact on the mesoscale morphology and mechanical properties.

In summary, we synthesized discrete, high-molar-mass, *it*-ABA all-PHA tri-BCPs with P3HB as the hard block and three types of soft midblocks: P3HV, P3HHp, and P3HBHp. The stereoselective ROP of *rac*-8DL$^R$ (R = Me, Et, and $^n$Bu) by complex **1** and di-initiator BDM is living and controlled, and the synthesis of the well-defined tri-BCPs was accomplished in two monomer-addition steps. The all-PHA tri-BCPs with a midblock mol % of greater than 50% still exhibit a high $T_m \sim$ 160 °C. While P3HB-*b*-P3HV-*b*-P3HB is a semicrystalline, strong, and tough thermoplastic, P3HB-*b*-P3HHp-*b*-P3HB is an elastomer with no observable yield point. On the other


https://doi.org/10.1021/acsmacrolett.3c00162
ACS Macro Lett. 2023, 12, 619−625

hand, P3HB-*b*-P3HBHp-*b*-P3HB exhibits the strength and elasticity in between the tri-BCPs with the P3HV and P3HHp midblock. The WAXS analysis of these tri-BCPs suggests that their varied mechanical properties are a result of the different degrees of crystallinity. Overall, the results obtained from this study further showcase the precision and tunability of the chemocatalytic route when applied to the all-PHA tri-BCP synthesis.

## ■ ASSOCIATED CONTENT

### Supporting Information

The Supporting Information is available free of charge at https://pubs.acs.org/doi/10.1021/acsmacrolett.3c00162.

Experimental methods and procedures, additional figures including SEC traces, $^{13}C$ NMR spectra, DOSY spectra, TGA curves, WAXS heating data, and additional tables (PDF)

## ■ AUTHOR INFORMATION


### Corresponding Author

**Eugene Y.-X. Chen** − *Department of Chemistry, Colorado State University, Fort Collins, Colorado 80523-1872, United States;* orcid.org/0000-0001-7512-3484; Email: eugene.chen@colostate.edu

### Authors

**Andrea H. Westlie** − *Department of Chemistry, Colorado State University, Fort Collins, Colorado 80523-1872, United States;* orcid.org/0000-0003-0003-2419

**Sarah A. Hesse** − *Stanford Synchrotron Radiation Lightsource, SLAC National Accelerator Laboratory, Menlo Park, California 94025, United States;* orcid.org/0000-0002-2383-4476

**Xiaoyan Tang** − *Department of Chemistry, Colorado State University, Fort Collins, Colorado 80523-1872, United States;* orcid.org/0000-0002-0050-6699

**Ethan C. Quinn** − *Department of Chemistry, Colorado State University, Fort Collins, Colorado 80523-1872, United States;* orcid.org/0000-0002-9609-806X

**Celine R. Parker** − *Department of Chemistry, Colorado State University, Fort Collins, Colorado 80523-1872, United States*

**Christopher J. Takacs** − *Stanford Synchrotron Radiation Lightsource, SLAC National Accelerator Laboratory, Menlo Park, California 94025, United States*

**Christopher J. Tassone** − *Stanford Synchrotron Radiation Lightsource, SLAC National Accelerator Laboratory, Menlo Park, California 94025, United States*

Complete contact information is available at: https://pubs.acs.org/10.1021/acsmacrolett.3c00162


### Author Contributions

E.Y.-X.C. conceived the project and directed research. A.H.W. designed and conducted experiments related to monomer and polymer synthesis as well as polymer characterizations. X.T., E.C.Q., and C.R.P. performed experiments related to monomer and polymer syntheses. S.A.H., C.J.Takacs, and C.J.Tassone performed WAXS experiments and analysis. A.H.W. and E.Y.-X.C. wrote the initial manuscript and revised subsequent versions of the manuscript, and all authors contributed to the revised manuscript.

### Notes

The authors declare no competing financial interest.

## ■ ACKNOWLEDGMENTS

This work was supported by the U.S. Department of Energy, Office of Energy Efficiency and Renewable Energy (EERE), Bioenergy Technologies Office (BETO), and Advanced Materials and Manufacturing Technologies Office (AMMTO). This work was performed as part of the BOTTLE Consortium, which includes the members from Colorado State University and SLAC, and funded under Contract No. DE-AC36-08GO28308. Use of the Stanford Synchrotron Radiation Lightsource, SLAC National Accelerator Laboratory, is supported by the U.S. Department of Energy, Office of Science, Office of Basic Energy Sciences under Contract No. DE-AC02-76SF00515. In the early stage of the PHA project, the work by X.T. and E.Y.-X.C. was supported by the U.S. National Science Foundation (NSF-1955482). We thank Dr. R. Clarke of the Chen group and Dr. R. Allen of NREL for assistance with polymer analyses.

## ■ REFERENCES


(1) Laycock, B.; Halley, P.; Pratt, S.; Werker, A.; Lant, P. The Chemomechanical Properties of Microbial Polyhydroxyalkanoates. *Prog. Polym. Sci.* **2013**, *38*, 536−583.

(2) Wang, Y.; Yin, J.; Chen, G.-Q. Polyhydroxyalkanoates, Challenges and Opportunities. *Curr. Opin. Biotechnol.* **2014**, *30*, 59−65.

(3) Müller, H.-M.; Seebach, D. Poly(Hydroxyalkanoates): A Fifth Class of Physiologically Important Organic Biopolymers? *Angew. Chem., Int. Ed.* **1993**, *32*, 477−502.

(4) Anjum, A.; Zuber, M.; Zia, K. M.; Noreen, A.; Anjum, M. N.; Tabasum, S. Microbial Production of Polyhydroxyalkanoates (PHAs) and Its Copolymers: A Review of Recent Advancements. *Int. J. Biol. Macromol.* **2016**, *89*, 161−174.

(5) Chen, G.-Q. A Microbial Polyhydroxyalkanoates (PHA) Based Bio- and Materials Industry. *Chem. Soc. Rev.* **2009**, *38*, 2434−2446.

(6) Anjum, A.; Zuber, M.; Zia, K. M.; Noreen, A.; Anjum, M. N.; Tabasum, S. Microbial Production of Polyhydroxyalkanoates (PHAs) and Its Copolymers: A Review of Recent Advancements. *Int. J. Biol. Macromol.* **2016**, *89*, 161−174.

(7) Arumugam, A. Polyhydroxyalkanoates (PHA) Production. *Encycl. Renew. Sustain. Mater.* **2020**, *2*, 236−252.

(8) Westlie, A. H.; Quinn, E. C.; Parker, C. R.; Chen, E. Y.-X. Synthetic Biodegradable Polyhydroxyalkanoates (PHAs): Recent Advances and Future Challenges. *Prog. Polym. Sci.* **2022**, *134*, 101608.

(9) Adamus, G.; Domiński, A.; Kowalczuk, M.; Kurcok, P.; Radecka, I. From Anionic Ring-Opening Polymerization of $\beta$-Butyrolactone to Biodegradable Poly(Hydroxyalkanoate)s: Our Contributions in This Field. *Polymers (Basel)* **2021**, *13*, 4365.

(10) Carpentier, J.-F. Discrete Metal Catalysts for Stereoselective Ring-Opening Polymerization of Chiral Racemic $\beta$-Lactones. *Macromol. Rapid Commun.* **2010**, *31*, 1696−1705.

(11) Li, H.; Shakaroun, R. M.; Guillaume, S. M.; Carpentier, J.-F. Recent Advances in Metal-Mediated Stereoselective Ring-Opening Polymerization of Functional Cyclic Esters towards Well-Defined Poly(Hydroxy Acid)s: From Stereoselectivity to Sequence-Control. *Chem.—Eur. J.* **2020**, *26*, 128−138.

(12) Lecomte, P.; Jérôme, C. Recent Developments in Ring-Opening Polymerization of Lactones. In *Adv. Polym. Sci.*; Rieger, B., Kunkel, A., Coates, G. W., Reichardt, R., Dinjus, E., Zevaco, T. A., Eds.; 2012; Vol. *245*, pp 173−217.

(13) Thomas, C. M. Stereocontrolled Ring-Opening Polymerization of Cyclic Esters: Synthesis of New Polyester Microstructures. *Chem. Soc. Rev.* **2010**, *39*, 165−173.

(14) Okada, M. Chemical Syntheses of Biodegradable Polymers. *Prog. Polym. Sci.* **2002**, *27*, 87−133.

(15) Tang, X.; Chen, E. Y.-X. Toward Infinitely Recyclable Plastics Derived from Renewable Cyclic Esters. *Chem.* **2019**, *5*, 284−312.

(16) Tang, X.; Chen, E. Y.-X. Chemical Synthesis of Perfectly Isotactic and High Melting Bacterial Poly(3-Hydroxybutyrate) from Bio-Sourced Racemic Cyclic Diolide. *Nat. Commun.* **2018**, *9*, 2345.
(17) Tang, X.; Westlie, A. H.; Watson, E. M.; Chen, E. Y.-X. Stereosequenced Crystalline Polyhydroxyalkanoates from Diastereomeric Monomer Mixtures. *Science* **2019**, *366*, 754−758.
(18) Tang, X.; Westlie, A. H.; Caporaso, L.; Cavallo, L.; Falivene, L.; Chen, E. Y.-X. Biodegradable Polyhydroxyalkanoates by Stereoselective Copolymerization of Racemic Diolides: Stereocontrol and Polyolefin- Like Properties Research Articles. *Angew. Chem., Int. Ed.* **2020**, *59*, 7881.
(19) Westlie, A. H.; Chen, E. Y.-X. Catalyzed Chemical Synthesis of Unnatural Aromatic Polyhydroxyalkanoate and Aromatic − Aliphatic PHAs with Record- High Glass-Transition and Decomposition Temperatures. *Macromolecules* **2020**, *53*, 9906−9915.
(20) Quinn, E. C.; Westlie, A. H.; Sangroniz, A.; Caputo, M. R.; Xu, S.; Zhang, Z.; Urgun-Demirtas, M.; Müller, A. J.; Chen, E. Y.-X. Installing Controlled Stereo-Defects Yields Semicrystalline and Biodegradable Poly(3-Hydroxybutyrate) with High Toughness and Optical Clarity. *J. Am. Chem. Soc.* **2023**, *145*, 5795−5802.
(21) Zhang, Z.; Shi, C.; Scoti, M.; Tang, X.; Chen, E. Y.-X. Alternating Isotactic Polyhydroxyalkanoates via Site- and Stereoselective Polymerization of Unsymmetrical Diolides. *J. Am. Chem. Soc.* **2022**, *144*, 20016−20024.
(22) Yang, J.-C.; Yang, J.; Zhang, T.-Y.; Li, X.-J.; Lu, X.-B.; Liu, Y. Toughening Poly(3-Hydroxybutyrate) by Using Catalytic Carbonylative Terpolymerization of Epoxides. *Macromolecules* **2023**, *56*, 510−517.
(23) Yang, J.-C.; Yang, J.; Li, W.-B.; Lu, X.-B.; Liu, Y. Carbonylative Polymerization of Epoxides Mediated by Tri-Metallic Complexes: A Dual Catalysis Strategy for Synthesis of Biodegradable Polyhydroxyalkanoates. *Angew. Chem., Int. Ed.* **2022**, *61*, No. e202116208.
(24) Wanamaker, C. L.; O'Leary, L. E.; Lynd, N. A.; Hillmyer, M. A.; Tolman, W. B. Renewable-Resource Thermoplastic Elastomers Based on Polylactide and Polymenthide. *Biomacromolecules* **2007**, *8*, 3634−3640.
(25) Wanamaker, C. L.; Bluemle, M. J.; Pitet, L. M.; O'Leary, L. E.; Tolman, W. B.; Hillmyer, M. A. Consequences of Polylactide Stereochemistry on the Properties of Polylactide-Polymenthide-Polylactide Thermoplastic Elastomers. *Biomacromolecules* **2009**, *10*, 2904.
(26) Martello, M. T.; Hillmyer, M. A. Polylactide-Poly(6-Methyl-ε-Caprolactone)-Polylactide Thermoplastic Elastomers. *Macromolecules* **2011**, *44*, 8537−8545.
(27) Schneiderman, D. K.; Hill, E. M.; Martello, M. T.; Hillmyer, M. A. Poly(Lactide)-Block-Poly(ε-Caprolactone-Co-ε-Decalactone)-Block-Poly(Lactide) Copolymer Elastomers. *Polym. Chem.* **2015**, *6*, 3641−3651.
(28) Watts, A.; Kurokawa, N.; Hillmyer, M. A. Strong, Resilient, and Sustainable Aliphatic Polyester Thermoplastic Elastomers. *Biomacromolecules* **2017**, *18*, 1845−1854.
(29) Liffland, S.; Hillmyer, M. A. Enhanced Mechanical Properties of Aliphatic Polyester Thermoplastic Elastomers through Star Block Architectures. *Macromolecules* **2021**, *54*, 9327−9340.
(30) Pederson, E. N.; McChalicher, C. W. J.; Srienc, F. Bacterial Synthesis of PHA Block Copolymers. *Biomacromolecules* **2006**, *7*, 1904−1911.
(31) McChalicher, C. W. J.; Srienc, F. Investigating the Structure-Property Relationship of Bacterial PHA Block Copolymers. *J. Biotechnol.* **2007**, *132*, 296−302.
(32) Li, S.; Cai, L.; Wu, L.; Zeng, G.; Chen, J.; Wu, Q.; Chen, G.-Q. Microbial Synthesis of Functional Homo-, Random, and Block Polyhydroxyalkanoates by β-Oxidation Deleted Pseudomonas Entomophila. *Biomacromolecules* **2014**, *15*, 2310−2319.
(33) Jaffredo, C. G.; Carpentier, J.-F.; Guillaume, S. M. Poly(Hydroxyalkanoate) Block or Random Copolymers of β-Butyrolactone and Benzyl β-Malolactone: A Matter of Catalytic Tuning. *Macromolecules* **2013**, *46*, 6765−6776.
(34) Hazer, B.; Akyol, E.; Şanal, T.; Guillaume, S.; Çakmakli, B.; Steinbuchel, A. Synthesis of Novel Biodegradable Elastomers Based on Poly[3-Hydroxy Butyrate] and Poly[3-Hydroxy Octanoate] via Transamidation Reaction. *Polym. Bull.* **2019**, *76*, 919−932.
(35) Kernbichl, S.; Reiter, M.; Adams, F.; Vagin, S.; Rieger, B. $CO_2$-Controlled One-Pot Synthesis of AB, ABA Block, and Statistical Terpolymers from β-Butyrolactone, Epoxides, and $CO_2$. *J. Am. Chem. Soc.* **2017**, *139*, 6787−6790.
(36) Adams, F.; Pehl, T. M.; Kränzlein, M.; Kernbichl, S. A.; Kang, J.-J.; Papadakis, C. M.; Rieger, B. (Co)Polymerization of (−)-Menthide and β-Butyrolactone with Yttrium-Bis(Phenolates): Tuning Material Properties of Sustainable Polyesters. *Polym. Chem.* **2020**, *11*, 4426−4437.
(37) Coulembier, O.; Mespouille, L.; Hedrick, J. L.; Waymouth, R. M.; Dubois, P. Metal-Free Catalyzed Ring-Opening Polymerization of β-Lactones: Synthesis of Amphiphilic Triblock Copolymers Based on Poly(Dimethylmalic Acid). *Macromolecules* **2006**, *39*, 4001−4008.
(38) Tang, X.; Shi, C.; Zhang, Z.; Chen, E. Y.-X. Toughening Biodegradable Isotactic Poly(3-Hydroxybutyrate) via Stereoselective Copolymerization of a Diolide and Lactones. *Macromolecules* **2021**, *54*, 9401−9409.
(39) Bruckmoser, J.; Rieger, B. Simple and Rapid Access toward AB, BAB and ABAB Block Copolyesters from One-Pot Monomer Mixtures Using an Indium Catalyst. *ACS Macro Lett.* **2022**, *11*, 1067−1072.




https://doi.org/10.1021/acsmacrolett.3c00162
*ACS Macro Lett.* 2023, 12, 619−625